이학석사학위논문

Estimation of Thermal Neutron Fluence by Monte Carlo Simulation and Experimental Measurement of TLD

몬테카를로전산모사와열형광선량계 측정을통한열중성자속추정

2019 년 8 월

서울대학교 융합과학기술대학원

융합과학부 방사선융합의생명전공

Ahmed Ibrahim Khalil

A Thesis for the Degree of Master of Science

Estimation of Thermal Neutron Fluence by Monte Carlo Simulation and Experimental Measurement of TLD

몬테카를로전산모사와열형광선량계 측정을통한열중성자속추정

2019 년 7 월

Program in Biomedical Radiation Sciences
Department of Transdisciplinary Studies
Graduate School of Convergence Science and Technology
SEOUL NATIONAL UNIVERSITY

Ahmed Ibrahim Khalil

Estimation of Thermal Neutron Fluence by Monte Carlo Simulation and Experimental Measurement of TLD

몬테카를로 전산모사와 열형광 선량계 측정을 통한 열중성자속 추정

지도교수예성준

이논문을 이학석사학위논문으로 제출함
2019 년 7 월

서울대학교 융합과학기술대학원
융합과학부 방사선융합의생명전공

Ahmed Ibrahim Khalil

카릴아흐메드의석사학위논문을인준함
2019 년 7 월

위 원 장**최희동(인)**

부위원장**예 성준 (인)**

위 원**김 기현(인)**

Estimation of Thermal Neutron Fluence by Monte Carlo Simulation and Experimental Measurement of TLD

By

Ahmed Ibrahim Khalil

A thesis submitted to the Department of Transdisciplinary Studies in partial fulfillment of the requirements for the Degree of Master of Science in Biomedical Radiation Sciencesat the Graduate School of Convergence Science and Technology

Seoul National University

July2019

Approved by Thesis Committee:

Chairperson: Hee Dong Choi (인)

Vice Chairman: Sung-Joon Ye(인)

Examiner: Geehyung Kim (인)

ABSTRACT

Estimation of Thermal Neutron Fluence by Monte Carlo Simulation and Experimental Measurement of TLD

Ahmed Ibrahim Khalil

Program in Biomedical Radiation Sciences

Department of Transdisciplinary Studies

Graduate School of Convergence Science and Technology

Seoul National University

In dosimetry, where it is necessary to measure (or estimate) the presence of thermal neutron fluxemanating from nuclear reactors, boron neutron capture therapy (BNCT) beam facilitiesand other neutron sources, the activation foil methodiscommonly used; however, it has the disadvantage of requiring a well-timed readout prior to the decay of the activation products as well asexpensiveHPGe detectors to count the emitted photons

from the irradiated sample.In addition, it is prone to noise from unwanted activation products.

The objective of this study is to present, evaluate and verify an alternative method that uses LiF based thermoluminescent dosimeters (TLD) to obtain thermal neutron fluence. This method is an alternative to the commonly used activation foil method.Thermoluminescence dosimeters are widely used in clinical settings to estimate photon and neutron doses andtheir response and characteristics have been well established.

This study evaluatedthe neutron flux spectrumemitted from a Cf-252 neutron source through a moderating shadow cone using Monte Carlo calculations, and then experimentally verified its dose deposition, and H*(10) ambient dose equivalent. To account for thermal neutron fluence, a cadmium sheet was folded to shield groups of TLDs from direct and scattered thermal neutrons in the experiment. It was possible to account for thermal neutron fluence by simply subtracting the shielded TLD dose reading from the unshielded onesbecause cadmium is an excellent shield against thermal neutrons. The shadow cone was used as a neutron moderator between the californium source and the TLDs; it thermalizes fast neutrons emanating from the californium source.

Monte Carlo simulations showed that a majority of energy deposit in TLD was caused by thermal neutrons and that scattered neutrons from the walls of this irradiation room were non-negligible and must be accounted for. The thermal neutron fluence calculated by Monte Carlo was converted into H*(10) ambient dose rate equivalent according to the ICRP recommendations, this was then verified against calibrated ^{3}He detector readings. The difference between Monte Caro and measured results wasless than 3.5%. The ratio of simulated thermal neutron fluence among position A (unshielded), position B (shielded in the front by a Cd sheet) and position C (shielded insidea folded Cdpocket) were in good agreement with experimental values obtained from TLD neutron dose readings at the same positions.

In conclusion, the developed method is sufficient as an alternative to the activation foil method to determine the thermal neutron flux for the pre-calibrated TLD system. Sincethe results from Monte Carlo simulations were in fair agreement with calibrated measurements, the method aided by Monte Carlo can be further used tocalibratethe TLD system.

Keywords: Thermal neutron flux, MonteCarlo, Cf-252 neutronsource, cadmium,thermoluminescence dosimetry.

Student Number: 2017-29551

List of Figures

List of Tables

CONTENTS

Introduction

In neutron beam dosimetry, where neutron fluence estimation is essential such as in fields of radiation protection, nuclear reactors, medical, and industrial sectors, the measurement of the neutron beam propertiesis essential. Nuclear reactions at nuclear power plants require neutrons to be thermalized to low energies in order to operate, whereas in the sector of Boron Neutron Capture Therapy, thermal neutron contribution is unwanted and should be minimized, in fact, the required ratio of thermal to epithermal neutrons in BNCT should ideally be 0.05 or less[1].Neutron beam dosimetry is a complex topicdepending on its field of use, according to the latest ICRP recommendation the radiation weighting factor for neutrons in tissue is taken as a continuous function of its energy[2].

There are many methods to measure neutron beam flux; activation foil method is known as the gold standard to measure neutron flux in the thermal, epithermal and fast neutron range[3]. Activation foil method consists of irradiating a sample at a high flux neutron beam and then measuring the radiation emitted from the decay of the activation products of that sample. The main advantage is that activation foil method is insensitive to photon irradiation. The main disadvantage lies in the

necessity of having a complicated setup requiring an expensive HPGe detector, with the limitation of positioning the detector far from background radiation. In addition, the irradiated activation foil has a specific decay half-life, this requires a well-timed period between irradiations and reading, and is susceptible to error caused by impurities in the sample.

There are other methods for measuring neutron beam profile, photon dose, energy spectrum, and dose rate, with some methods being more established than others. A well-established method for neutron dosimetry is the use of thermoluminescent dosimeters (TLD). Thermoluminescent dosimeters store the energy imparted from radiation dose in metastable electronic bands in the TLD material, during reading, the TLDs are heatedand the energy is released as visible light emission, the amount of light emitted is proportional to the imparted radiation dose, the TLD reader counts the lights and allows for dose estimation. Depending on their composition, TLDs have a different response to neutron or gamma radiation. LiF based TLDs are a well-established radiation measurement method and are nearly tissue equivalent and not as susceptible to temporal variation between irradiation and reading, they do not require a very expensive setup, and can simultaneously measure neutron and photon contribution. Theoretically, the cross-section of ^{6}Liis higher than gold

used in activation foil dosimetry, this indicates that ^{6}Li based TLDs are more sensitive than gold foil method in the thermal neutron range.In this study, pairs of TLD-600 and TLD-700 chips are employed as they have a different response to neutrons, with TLD-600 being neutron sensitive and TLD-700 being neutron insensitive,Both TLDs have a similar response to photons. It is possible to obtain the neutron dose by simply subtracting the dose reading of TLD-700 from TLD-600. A cadmium sheet is often employed in order to shield pairs of TLDs from thermal neutrons, thermal neutrons are low energy neutrons below cadmium's energy cutoff that extends up to 0.4 eV, by using the simple ratio method of shield TLDs to unshielded TLDs, it is possible to obtain the thermal neutron contribution.

The purpose of this study is to evaluate and establishlithium fluoride based thermoluminescence dosimeters, specifically TLD-600 and TLD-700 as an alternative methodto estimate thermal neutron fluence byusing numerical and experimental methods. We propose this method as an alternative to the complicated gold foil activation method. This study aims to prove TLDs as a capable and accurate method in estimating thermal neutron fluence in mixed neutron and photon fields by using pairs of TLDs and a cadmium sheet. First, Monte Carlo simulation is used to estimate the spectrum and neutron fluence, and then by comparing it to experimentally exposing the TLDs to a californium-252 neutron source in

a similar geometry to the Monte Carlo simulation to obtain thermal neutron fluence.This study will allow to measure the thermal neutron fluence and verify it by cross-calibration between numerical and experimental methods, finally, the simulated ambient dose rate is experimentally compared with calibrated instrument measurement.

Theory

2.1 TLD response

Thermoluminescent dosimeters are commonly used and are well established for neutron dosimetry. TLDs have a different response to neutrons depending on their component materials' cross-section.The dosimeters usedin this study are LiF based TLD-600 and TLD-700dosimeters; they were procured from ThermoFisher scientific.TLD-600, which is mainly composed of ^{6}Li (95.6%) enriched LiFand some ^{7}Li(4.4%). And TLD-700is mainly composed of ^{7}Li(99.99%) enriched LiF and trace amounts of ^{6}Li. TLD-600 is sensitive to neutrons mainly due to the high cross-section of its component ^{6}Li. Whereas TLD-700 is insensitive to neutrons due to the lower cross-section of its component ^{7}Li. To evaluate the thermal neutron dose contribution, a Cadmium sheet was used to shield a batch of TLDs from direct thermal neutrons as cadmium has ahigh cross sectional cutoff for neutrons with energy below 0.5 eV. Figure 1 shows the cross-section of ^{6}Li and ^{7}Li and Cadmium[3].The atomic response to neutronsin TLDs to be known is the product of the reaction probability (cross-section) and neutron fluence as shown in equation 1

Equation 1 the reaction rate per atom to neutron fluence

$$R = \int \sigma(E)\Phi(\mathrm{E})\ \mathrm{dE}$$

The dose response of the TLDs to neutrons is analytically estimated using equation 2, wherein $D_{(n,\alpha)}^{TLD}$ is the dose imparted in a TLD from ^{6}Li (n,α) reaction, Q_1 is the energy dissipated from the (n,α) reaction, $\rho 1$ is the material's density, N_{Li-6} is Avogadro's number of ^{6}Li atoms and $\bar{\sigma}_{(n,\alpha)}^{Li-6}$ is thefluence weighted microscopic cross-section of ^{6}Li, and ϕ_{th} is the thermal neutron fluence.

Equation 2 dose imparted by a known neutron beam in TLDs

$$D_{(n,\alpha)}^{TLD} = Q_1 \times \left(\frac{1}{\rho_1}\right) \times N_{Li-6} \times \bar{\sigma}_{(n,\alpha)}^{Li-6} \times \phi_{th}$$

Whereinthe definition of ϕ_{th} is defined as below:

$$\phi_{th} = \int_0^{0.4\ eV} \varphi(E)\quad dE$$

The average cross-section of TLD-600 is given by equation 3. The ratios of averaged cross-sections were calculated accordingly using MATLAB®trapezoidal integration function, the neutron fluence was obtained using MCNP calculation and the microscopic cross-section from ENDF/VII.1[3], thecross-section data integrated in the thermal region (zero to 0.4 eV).

Equation 3 shows the average cross-section obtained using thermal neutron fluence, φ symbolizes thermal neutron fluence at each position

$$\overline{\sigma} = \frac{\int_0^{0.4\ eV} \sigma(E) \cdot \varphi(E) \quad dE}{\phi_{th.}}$$

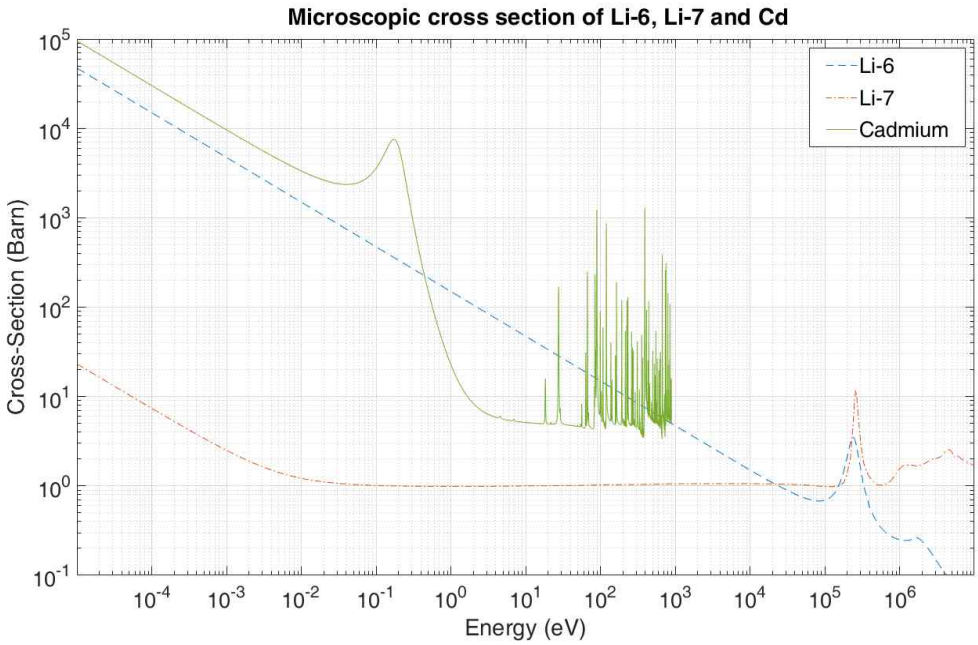

Figure 1cross-section of Li-6, Li-7, andcadmium

2.2 Californium source

In this study, a californium-252 source was used to irradiate the TLDs,californium decays by α emission to curium-248 (96.9%) and by spontaneous fission (3.1%) emitting 3.768 neutrons and 7.98 photons per spontaneous fission, with average neutron energy of 2.13 MeV[4] the gamma rays accompany its α decay as well as in spontaneous fission. However, the gamma emission realistically differs based on the age of the source and it is affected by the neutron-induced inelastic collision and capture gamma reactions with materials in the testing facility[5] , also, the daughter nuclei of the source emit gamma rays themselves and contribute to the source's gamma emission.Despite its high photon emission strength, the neutron dose contribution of cf-252 is much higher than its photon dose. cf-252 has a specific activity of 536 μCi/μg,due to its relatively high-energy neutron emission;either a shadow cone or a heavy water sphere usually moderates the emitted neutrons. For this study, a stainless steel /polyethylene shadow cone was used to moderate the emitted fast neutrons[5]. Figure 2 shows the decay scheme of cf-252.

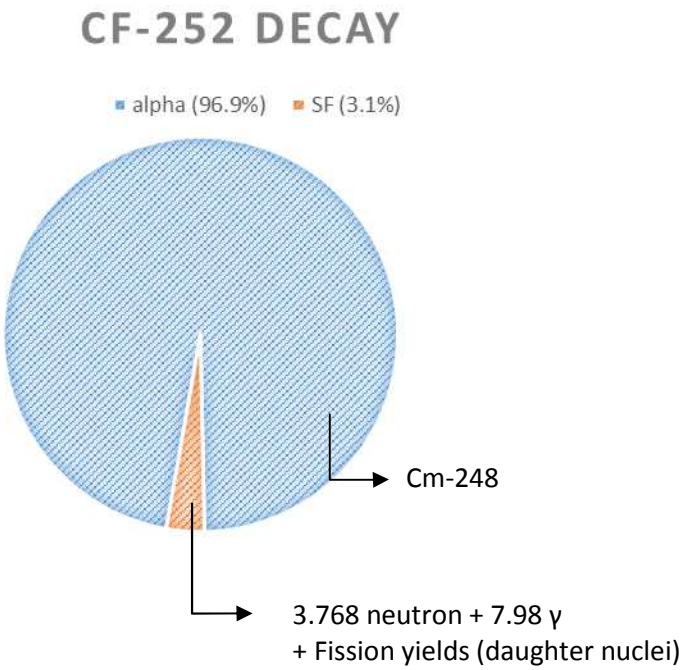

Figure 2decay scheme of cf-252

For the simulation of the source to be conducted using MCNP 6.1, a Watt fission spectrum (equation 4) was used from the LLNL fission model with parameters *a=1.025 b=2.926* according to the MCNP manual [6]. To simulate gamma ray emissions, the LLNL fission model was used by adding *FMULT METHOD=5* to the input file for simulation. The raw californium spectrum was first simulated in a point source geometry; the spontaneous fission multiplicity of Cf-252 that was obtained using MCNP is shown in figure3.

Equation 4 Watt equation describing Cf-252 energy spectrum

$$N(E) = e^{-\frac{E}{a}} \sinh\left(\sqrt{bE}\right)$$

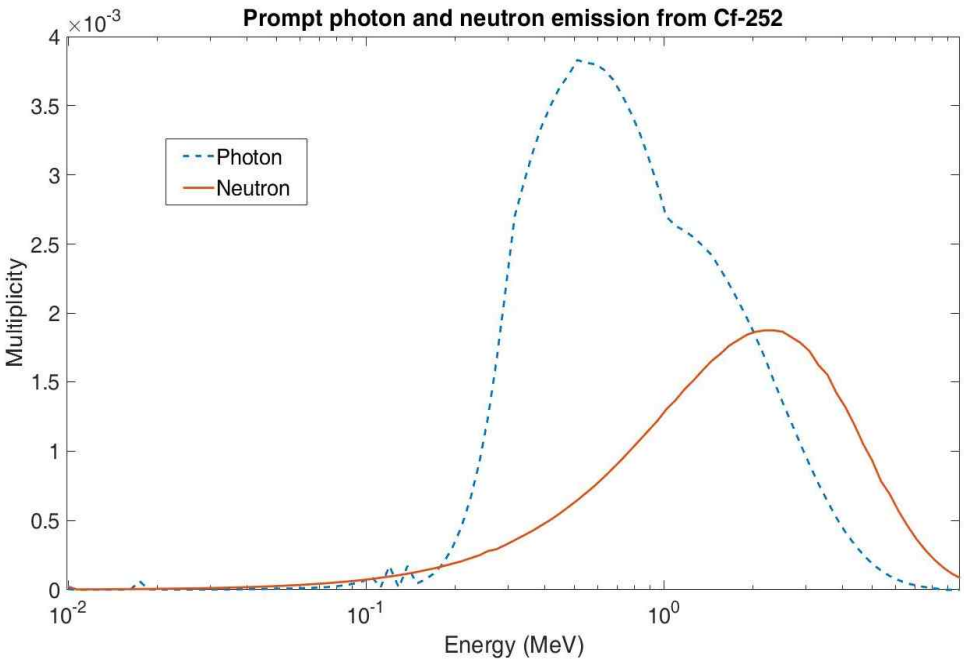

Figure 3 photon and neutron multiplicity of Cf-252 prompt emission

A 50 cm long polyethylene/stainless steel cone was used to moderate the fast neutrons emitted from the source, the use of a polyethylene shadow cone is in order to thermalize the fast neutrons to the thermal range. Figure 4 shows a comparison between bare californium-252 neutron spectrum and shadow cone moderated spectrum.

The californium source used to irradiate the TLDs is a commercially procured Eckert & Ziegler 3036 californium source, the source is encapsulated in a stainless steel cylinder measuring 10 mm high × 7.8 mm in diameter [15]. It had an original activity of 1mCi at the reference date of 15 December 2015. A standard calibration measurement was done on 1st of July 2018, showing a neutron release rate of 2.073×10^{6} neutron per second. By simply following the decay formula, it is estimated that the neutron emission at the irradiation date 23 January 2019 to be 1.789×10^{6}neutron per second.

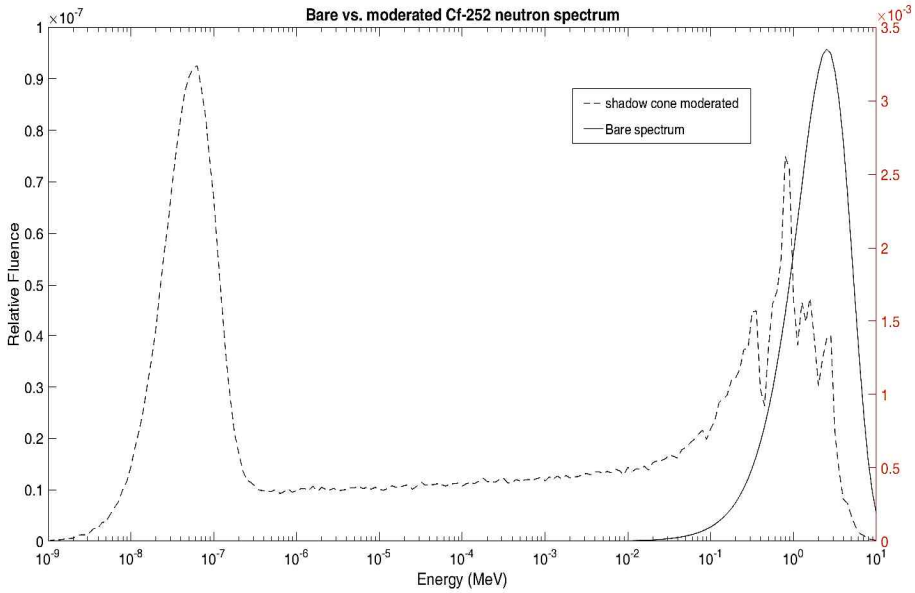

Figure 4 bare californium source spectrum and the shadow cone moderated spectrum

2.3ThermoluminescenceDosimeters

Thermoluminescence dosimeters respond to radiation when the valence band electrons of the impure crystal lattice in the TLD material are excited. The electrons move to the conduction band and are stuck in metastable levels in their outer shell electron orbitals (known as forbidden gap)[7]. The product are metastable electron trap centers, these electronic levels are unstable and upon heating or the addition of vibrational energy, the electrons return to their original shell orbital producing visible light,the amount of trap centers or luminescence centers are correlated with the increase in ionizing radiation[8].Upon heating the TLDs, the electrons return to their original position emitting visible light, the visible light is then detected using a photomultiplier tube and then counted using a TLD reader. The individual thermoluminescence dosimeters have varying sensitivity to radiation as minute differences in their composition leads to considerable difference in their sensitivity and efficiency, hence the need for calibration. Ideally, the element correction coefficient (ECC) for each TLD should be taken and accounted for, this is done by first exposing the TLDs to a known radiation field from a calibrated source, then the ECC is obtained by correlating the reading of the individual TLD to the actual calibrated read dose (or averaged dose). Then theReader calibration Factor (RCF) of the TLD reader should also be accountedfor; in that

case,the RCF eliminates any noise from the reader's Photomultiplier Tube (PMT).

2.4 Ambient dose rate

Ambient dose equivalent rate is an operational quantity used for area monitoring that is produced by the aligned radiation field at a depth of 10 mm in an ICRU tissue equivalent sphere with a diameter of 300 mm in an isotropic radiation field.

H*(10) is the product of particle fluence and a conversion coefficient given by equation 5, hence it relies on the energy dependent conversion factor. The conversion factor of E/Φ as a function of energy shows that over a wide energy range, thermal and slow neutrons impart little effective dose compared with fast neutrons, and since that in this field, fast neutron fluence does not change significantly between positions A,B and C, then, little ambient dose change is expected. Figure 5 shows the effective dose conversion coefficient between fluence and effective dose of neutrons as published by ICRP[9]

Equation 5 ambient dose equivalent conversion equation from ICRP

$$H* = \int h_{Em\ ax}(E)\Phi(E)dE$$

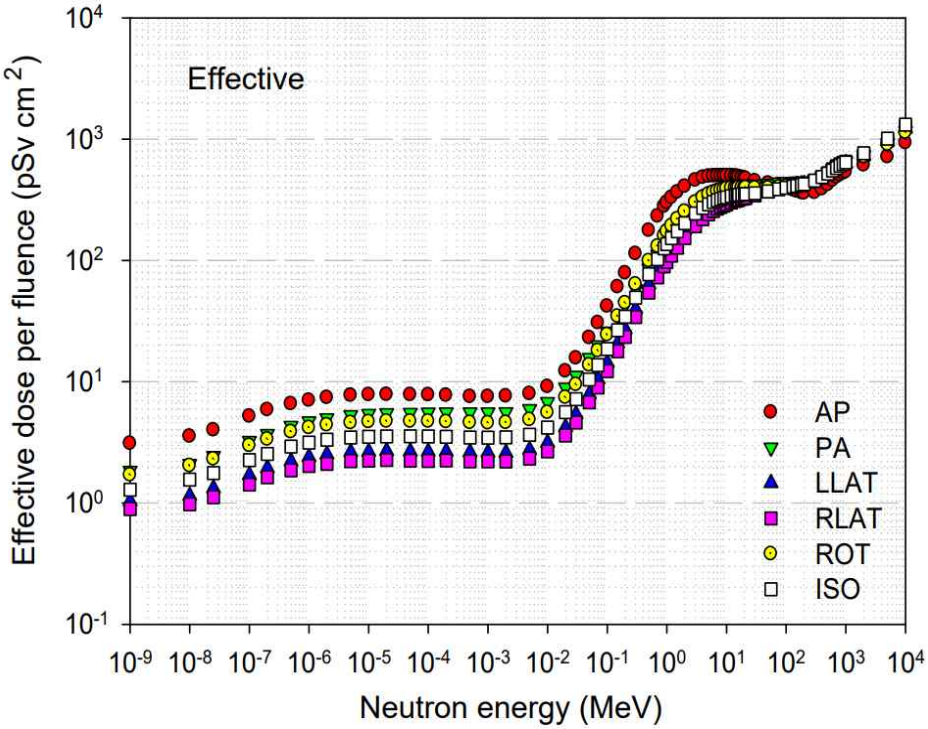

Figure 5 effective dose conversion coefficient from ICRP, 2010[9]

Materials and Methods

3.1 Experimental setup

3.1.1 Annealing

Annealing is a normal procedure prior to irradiating TLDs, this is done to eliminate any residual signal from previous irradiation or accumulated background dose.Before the irradiation, all TLDs were fully annealed in a Changshin science ceramic furnace at 400°C for one hour, then at 100°C for two hours as generally recommended for LiF dosimeters[8], the TLDs were left to cool overnight before irradiation began.

3.1.2 Irradiation

A total of 160 TLDs were taken to the irradiation room for irradiating at Pohang University of Science and Technology's (POSTECH) neutron irradiation room, there, a californium-252 neutron source is situated in a neutron irradiation room. The irradiation was started and was continued for exactly 48 hours. The TLDs were placed at 1 meter away from the source facing a 50cm long polyethylene/stainless steel shadow conein the front, the shadow cone thermalizes fast neutrons emitted from the californium source, but also attenuates the neutron fluence. 20 TLD-600

and 20 TLD-700 were left outside the irradiation room in a nearby office for background readings. Figure 6show a photograph of the irradiation room at POSTECH.

Figure 6 a photograph of the irradiation setup showing the californium source, shield, shadow cone, and cardboard TLD holder

3.1.3ThermoluminescenceDosimeters

The thermoluminescent dosimeters used in this study were lithium Fluoride based dosimeters, commonly known as TLD-600 and TLD-700, these TLDs were commercially procured from ThermoScientific™, all the TLDs were in the shape of a disk measuring 4.5 × 0.89 mm[10]. LiF;Mg,Tiis commonly used in dosimetry as its effective atomic number of 8.14 may be considered close to that of tissue (7.4), LiF makes up the most of the mass of the TLDs at around 99%, with the dopants Mg making up 200 ppm and Ti around only 10 ppm. TLD-600 and TLD-700 are commonly used in dosimetry to obtain photon and neutron dose[11] the main difference between the TLD-600 and TLD-700 is their lithium isotope composition, TLD-600 is mainly made up of 95.6% ^{6}Liand 4.4% ^{7}Li. TLD-700 is mostly composed of 99.99% ^{7}Li with trace amounts of ^{6}Li. The two types of detectors have a different sensitivity to neutrons because of their lithium isotope composition[8]. Table 1 shows mass composition fraction of each TLD type. During the irradiation,120 TLDs were placed in a cardboard holder and held facing the neutron source using scotch tape, this was done to reduce the perturbing effect of the holder on the neutron field. Each batch of TLDswascomposed of groups of 20 TLD-600 and 20 TLD-700, the first batch was directly exposed to the moderated neutron beam (position A), the second batch was shielded

in the front by a cadmium sheet (position B), and the third batch was placed inside a folded cadmium sheet pocket (position C).Figure7shows a schematic of how the TLDs were placed in relation to the neutron beam as visualized using MCNPX[12].

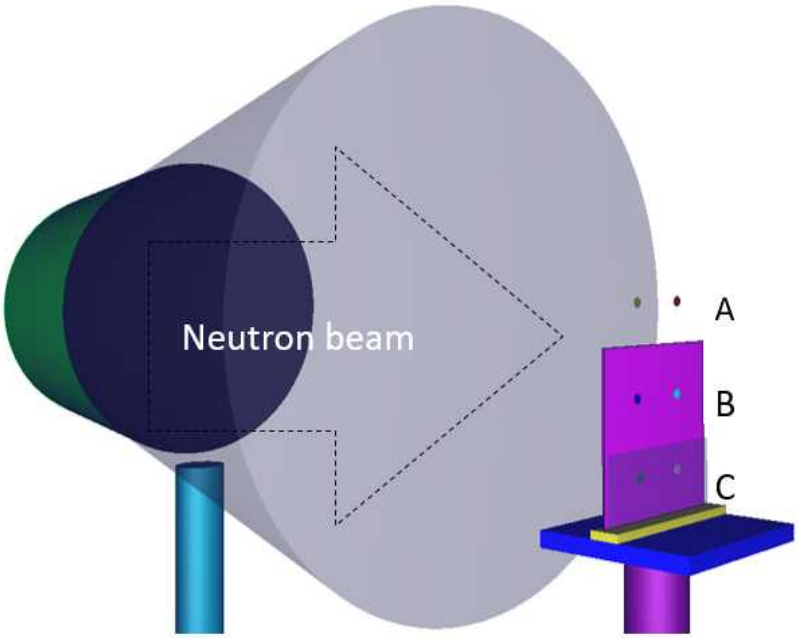

Figure 7visualization using MCNPX showing TLDs positioned in relation to the neutron beam with the front facing cadmium sheet colored violet and the back of the plate (folded part) being transparent grey,the left column of chips represents TLD-600, the right column represents TLD-700 chips.

	% lithium		Total Li	F	Mg (ppm)	Ti (ppm)	Density g/cc
-	^{6}Li	^{7}Li					
TLD-600	95.6	4.4	0.2676	0.732	200	10	2.55
TLD-700	0.001	99.99	0.2676	0.732	200	10	2.65

Table 1material composition of each TLD type used

3.1.4 Cadmium sheet

In a neutron irradiation setup, wherever there is a necessity to measure thermal neutrons, cadmium is commonly used as a shield from thermal neutrons. That isbecause of its sharp energy cutoff to thermal neutrons (20,600 barn) [11], cadmium's cross-sectionis high in the thermal neutron range and decreases sharply at neutron energies above 0.5 eV and above, it also shows some resonance at energies above 100 keV[3]. In this study, a 100 × 100 × 1 mm thick cadmium sheet was used to shield the TLDs from thermal neutrons from the source. In published articles, it is shown that scattered neutrons from walls have a non-negligible dose contribution, and that its fraction to the total neutron dose increases with increased distance from the neutron source [13, 14]. Hence, the cadmium sheet was folded at 2 cm from one of its edges with TLDs inside its folded pocket to account for the scattered neutrons from the walls of the irradiation room. The TLDs were either assembled to be above the cadmium sheet to be directly exposed to the thermalized neutron beam (Position A), behind the cadmium sheet (Position B) or shielded inside a folded cadmium pocket (Position C).

3.1.5Post-irradiation reading

The TLDs were read the same evening after the irradiation was completed. A Harshaw 3500 TLD reader was used, first, the background noise of the reader was accounted for, as well as dark readings, and then an optimal Time Temperature Profile (TTP) was selected for the reading according to the manual [15].The reader TTP was to first preheat TLDs to 50°C then linearly heat the TLDs until reaching 260°C, the acquisition time was set to be 26 2/3 second and heating rate was 10 °C/s, the output shows a glow curve spanning over 200 channel points. The readerhas a planchet heater and uses a PMT tube to read the thermoluminescence emitted from the TLDs, the data and glow curves are then sent via serial connection to an adjacent computer. All the TLDs were individually read and labelled using the same TTP.

3.1.6 Helium-3 detector readings

Ambient dose equivalent is an operational quantity widely used to measure the dose equivalent which would be generated at a depth of 10mm in a 300mm diameter tissue equivalent ICRU sphere, the unit for ambient dose rate equivalent is Sv/h. H*(10) ambient dose equivalent is commonly used for monitoring and assessing effective dose[2].

A calibrated ^{3}He detector instrument was used to obtain the ambient dose rate equivalent at the same position as the TLDs after they were irradiated. The Berthold technologies® LB-6411 is an H*(10) calibrated neutron probe, the probe is calibrated for the measurement of H*(10) ambient dose equivalent as published in ICRP-74[16]. The instrument measured the ambient dose rate to be 3.460 μSv/h, a value averaged from 13 measurements after subtracting the averaged background reading of 0.138 μSv/h.

3.2 Monte Carlo simulation

Monte Carlo numerical analysis was conducted using MCNP6.1[17], a general purpose code used for neutron, photon or coupled transport. All cross-section data used were evaluated from ENDF/B-VII.1[3], the MCNP calculations were carried on Intel Xeon® E5-2640 parallel processing units with a total of 50 processing threads. MCNP was used to tally the dose deposition in the TLDs using F6 tally (Energy deposit in MeV/gram), F4 tally (neutron fluence in #/cm²) was also used to obtain the neutron fluence in the TLDs placed directly behind the shadow cone, behind a cadmium sheet, and inside a folded cadmium sheet pocket. Special cross-sections are necessary to account for the material binding energy's effect on low energy neutron collisions, this material treatment was included by using MT card, material treatment was used whenever possible for Aluminum, Hydrogen in polyethylene, steel, and Hydrogen in concrete[18]. The used input cards for dose deposition are shown in Appendix A. To estimate the ambient dose rate equivalent H*(10), Dose Function card (DF) was used with F4 tally to convert fluence to dose rate in μSv/h as in ICRP recommendations[9]. The simulation was continued for 3×10^9 histories and until the resulting tally error was less than 0.05

3.2.1 Room Geometry

The simulation geometry of the actual irradiation room at POSTECH and the position of the TLDs were replicated using SimpleGeo[19].The inner room measurements are 830 × 640 × 410 cm, the room has 50 cm thick concrete walls, and the major components believed to affect scatter were all simulated in the irradiation room, these are the steel source shield, the irradiation pole, the shadow cone and holder as well as the stand for holding the samples to be irradiated. Other small components in the room were not included in the geometry; figure8a, shows a 3D visualization of the neutron irradiation room at POSTECH, b shows a cross-sectional view of the neutron irradiation room as visualized using MCNPX.

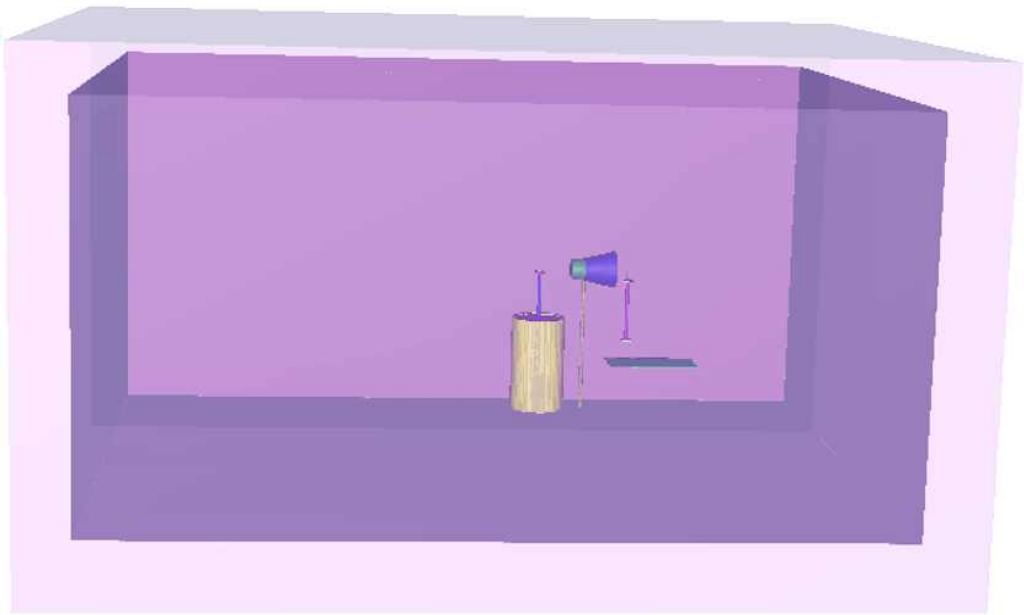

Figure 8 3D visualization of the irradiation room visualized using SimpleGeo software

Results

4.1 Simulation results

4.1.1 Neutron spectrum

MCNP simulation using F4 tally at the location of the TLDs placed in front of the beam, were obtained using 199 logarithmically separated energy bins.The position of the TLDs directly exposed to the moderated beam (A), behind a cadmium sheet (B), and inside a folded cadmium pocket (C) were evaluated, the shadow cone-moderated neutron spectrum is shown in figure 9.

Results in (A) are comparable to that of studies simulating neutron spectrum from a moderated californium 252 source in air. [14, 20] evaluated the scattered neutron contribution using simulation, by removing the scattering walls and simulating a pure source in vacuum without walls and subtracting it from a scattering room geometry.This is not realistically possible in this casesince this is an experimental study that is further verified by MCNP calculations.

The moderator increases the thermal neutron fluence below 1 eV. The spectrum shows a maximum peak at around 0.05 eV, however, the scattered neutron contribution in this case is non-negligible, and seems to

account fornearly halfof thermal neutron contribution; it is believed to be caused by inelastic collision with the room walls and ambient atmosphere.

The fast neutron region peak of the spectrum is not smooth as a Watt spectrum;it is caused by the known resonance at high neutron energies with the stainless-steel part of the shadow cone that attenuates the spectrum according to its cross-section.

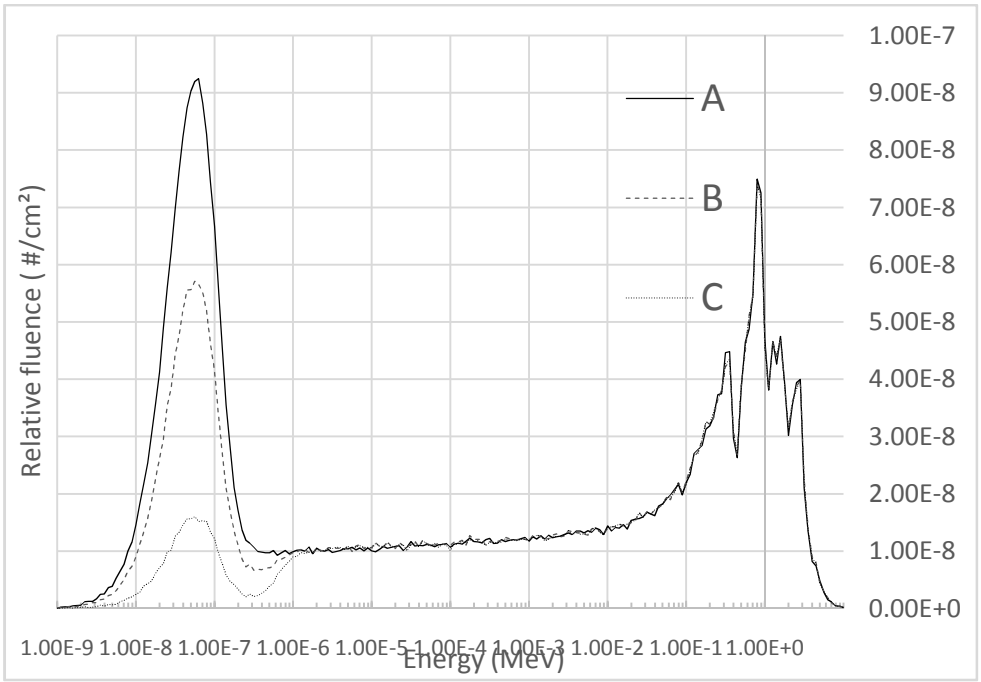

Figure 9Simulated neutron spectrum in TLDs using MCNP

4.1.2 Thermal neutron fluence

It is widely adopted that thermal neutrons are neutrons with energy of around 0.025 eV at S.T.P [21]the definition of thermal neutrons extends to 0.2 eV depending on the usage [22], however, cadmium's energy cut-off is 0.4 eV, therefore in this study neutrons with energy below 0.4 eV are taken as thermal neutrons. Thermal neutron contribution was integrated to obtain the total thermal neutron fluence at the positions previously mentioned from zero to 0.4 eV.Table 2 shows the ratios of thermal neutron fluence per history obtained using MCNP simulation normalized to unshielded TLD (position A).Dose modifier card (DF) was used, the parameter card used was *DF0 IC 40 IU 2 LOG FAC -1,* this parameter multiplied the calculated neutron fluenceand converted it using ICRP-60 flux-to-dose conversion coefficients.The result is the ambient dose rate equivalent in units of Sv/h [9], the result of dose rate yielded 3.585 μSv/h at position A TLDs, and 3.093 μSv/h at position B TLDs, and 2.956 μSv/h at position C TLDs.

Table 2ratio of thermal neutron fluence (zero to 0.4 eV) per history at TLD positions A, B, and C

TLD position	Thermal n/cm²/history	Normalized to (A)
A	1.8569E-6	**1**
B	8.6859-07	**0.467**
C	4.610E-08	**0.024**

4.1.3 Simulated neutron dose

The neutron dose at the three TLD positions in TLD material composed of ^{6}LiF for TLD-600 and ^{7}LiF for TLD-700 were evaluated using F6 tally to yield neutron energy deposition in MeV/gram. Figure10 shows that the neutron energy deposition in TLD-600 in position A is the highest and that a majority of neutron energy deposit in TLDs is in the thermal region (below 0.4 eV) as expected,since the cross-section of ^{6}Li is highest in the thermal neutron energy range. Simulation shows that the cadmium sheet attenuated the thermal neutrons well in position B TLDs and thatthe cadmium folded pocket TLDs in position C show little response, which is expected as cadmium shields thermal neutrons.Furthermore, some low energy epithermal neutrons (1-100 eV) caused some energy deposition in all TLDs, this is because the cadmium's cross-sectiondecreases sharply only below after 1 eV as energy increases and that the cross-section of Li-6 steadily decreases with increased neutron energy. According to these results, the highest thermal neutron dose contribution in TLD-600 position A is expected, followed by nearly half the dose contribution in TLD-600 at position B, and around a tenth of the first at position C. Dose contribution in TLD-700 chips is nearly negligible from neutron irradiation.

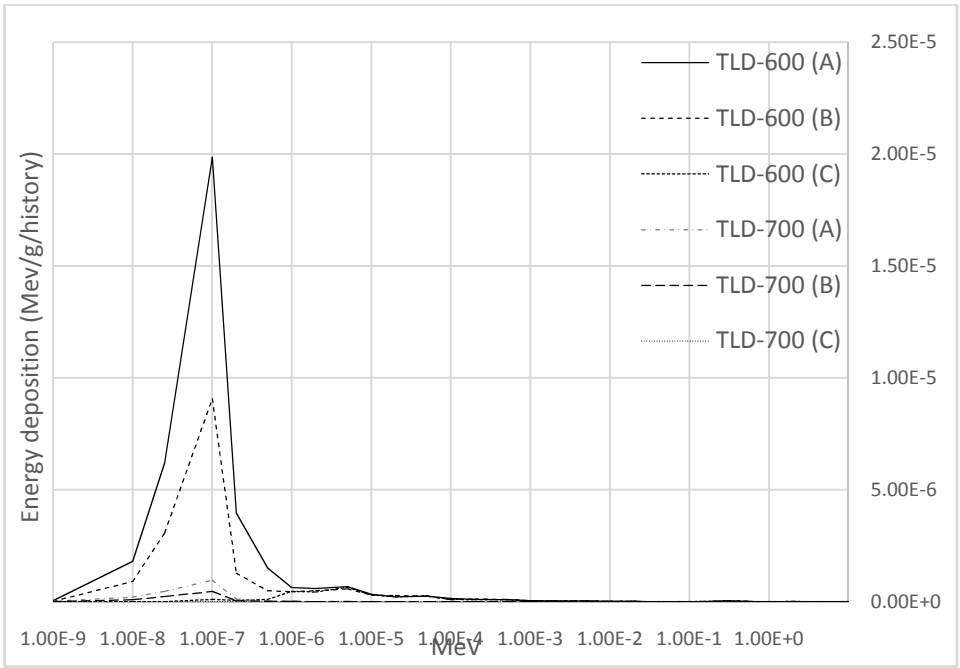

Figure 10simulated neutron energy deposition in TLDs

Table 3simulation results using MCNP tallies F4 and F6

-	Simulation			
label	MeV/g/n/history	Normalized[1]	Thermal n/cm²/history	Normalized[1]
A	3.34E-05	**1.000**	1.8569E-6	**1.000**
B	1.48E-05	**0.443**	8.6859-07	**0.467**
C	2.69E-07	**0.0806**	4.610E-08	**0.024**
Thermal neutron fluence n/cm²/history	Direct Thermal (A- B)	**9.883E-7**	Total thermal (A-C)	**1.8108E-6**

[1] normalized to position A

4.2 Experimental results

Glow curve shape and experimental data was obtained using WinRems™, a software provided with the Harshaw 3500 TLD reader. The raw glow curve data was acquired then exported in comma separated values to Microsoft Excel software for averaging and calculations.The averaged glow curve of TLD-600 and TLD-700 chips in positions A, B and C are shown in Figure11 and figure 12 respectively.The main peak at starting at channel 16 peaking at channel 52 and decreasing until channel 66 was chosen as the main Region Of Interest (ROI), smaller peaks appear at channels 85 and 103, however, these were neglected as high temperature peaks also shows at channels 103 and channel 145 in both TLD-700 and TLD-600.High temperature peaksare the result of neutron irradiation on TLD-700 [23].

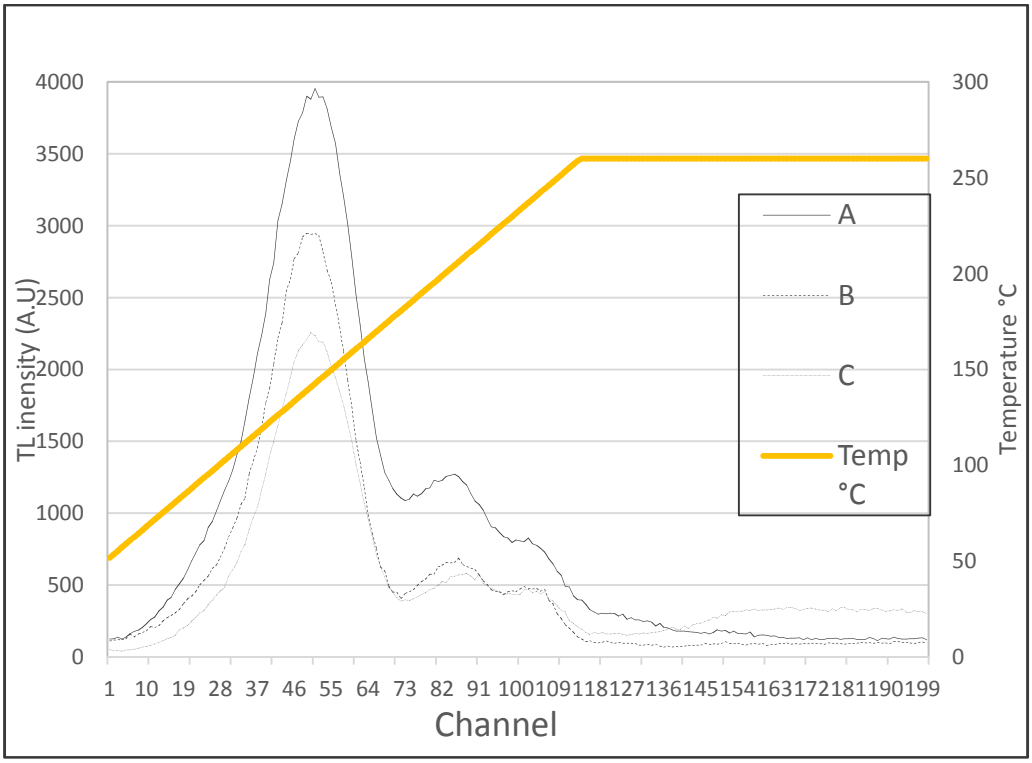

Figure 11averaged glow curve of TLD-600 disks after neutron irradiation

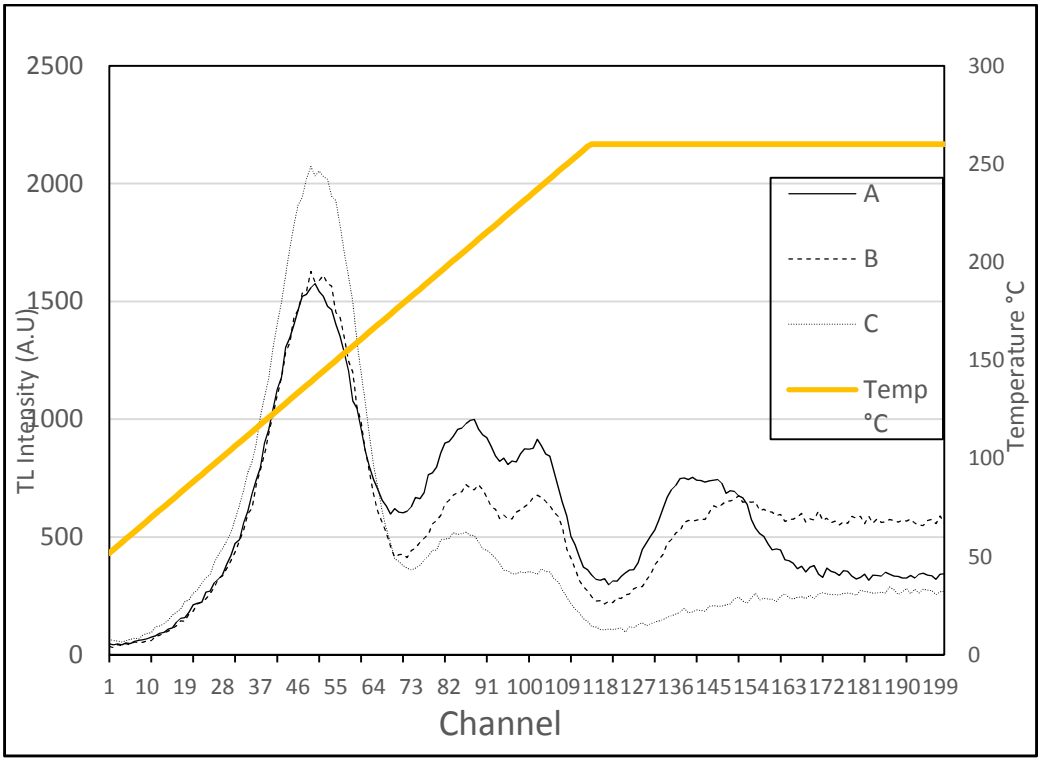

Figure 12averaged glow curve of TLD-700 disks after neutron irradiation

4.2.1 Sources of error

Thermoluminescence dosimetry is a three-step method that requires annealing, irradiation and reading, many errorsmay arise duringthis process, in TLD reading the errorscan be defined as systemic and random errors,bothcome from either the TLD chip or the TLD reader, all these factors add uncertainty to the dosimetric reading. The systemic errors may result from the annealing procedure, irradiation setup,and reader error or background noise. Fluctuation in the heating rate are alsoconsidered as systemic errors.TLD systemic errors occur due to the difference in the TLD chip composition, mass, or optical properties,also,any contamination or scratches on its surface causes difference in its dosimetric response. Random errors are the result of non-reproducibility of the position of the TLD in the reader tray or due to poor thermal contact between the TLDs and the heater[8]. Random errors alsoarise from inconsistency in the reading procedure by the user. All these factors contribute to uncertainty in the dosimetry procedure; the combined uncertainty arising from these errors (CU) is given in equation 6. In this study it was observed that 4 out of 5 TLDs that showed spurious readings were of the TLD-600 type in position A, these showed the highest standard deviation compared to the other groups or TLD-700 chips, to be as objective as possible, the 5 TLD readings were omitted

according to Chauvenet's criterion[24].Itis postulated that this error can be due to cross talk between the TLDs positioned too close together. Alpha particles are emitted in the TLD chip volume due to the ^{6} Li (n,α) reaction with a total energy of 4.78 MeV, it is possible that the generated alpha particles strike the neighboring TLD that was positioned nearby and impart additional dose. To further support this, the over-responsive TLDs were irradiated with X-rays only and compared with averaged TLD readings, no significant difference between those TLDs was found, this supports the theory of TLD cross talk when irradiated by neutrons. Table4 shows the average readings and standard deviation of each TLD group for TLD-600 and TLD-700 at positions A, B and C.

$$\text{CU}= \sqrt{(U_{Reader})^2 + (U_{user})^2 + (U_{TLD})^2}$$

Equation 6Non-exhaustive combined uncertainty that is the combined root sum square of TLD reader uncertainty, user uncertainty and TLD uncertainty.

Table 4 comparison of the average TLD readings, standard deviation, and variance for each TLD group at positions A, B and C.

-	Mean(in A.U.)		% S.D.		Variance (in A.U.)	
	TLD-600	TLD-700	TLD-600	TLD-700	TLD-600	TLD-700
A	8.19	3.85	75.43	27.74	18.51	1.141
B	5.36	3.13	26.90	34.02	2.079	1.334
C	3.78	3.29	33.70	34.04	1.780	1.135

4.2.2Experimental neutron dose

The main peak from neutron irradiation is visible in the low temperature region between channels 16 – 66. The TLD reader glow curve of TLD-600 is much more pronounced and visible as it received significant dose, whereas TLD-700 glow curve shows a non-smooth curve as the TLD reading is prone to noise and statistical uncertainty due to its small value that is comparable to background radiation. Integrating the area under the curve of ROI in TLDs positions A, B, and C shows that the cadmium sheet is excellent at shielding neutrons in the thermal range, and knowing that most of the energy deposited in TLDs is from thermal neutrons,itis estimated that nearly half of the neutron deposit in TLDs at position A is from scattered neutrons because the TLDs in position B received only scattered neutrons from the walls. The TLDs at position C accumulated neutron dose from epithermal and fast neutrons with energy above cadmium's energy cutoff, thus subtracting reading C from A yields total thermal neutron contribution. Table 5 shows the accumulated luminescence signal from averaged TLD readings normalized to position A as well as the experimentally obtained neutron dose reading.

Table 5experimentally obtained signal values from TLD readings

-	Experimental			
label	TLD-600 signal A.U.	TLD-700 signal A.U.	Neutron signal A.U.	Normalized
A	8.19	3.85	4.34	**1.000**
B	5.36	3.13	2.23	**0.514**
C	3.78	3.29	0.49	**0.113**
Signal A.U.	Direct Th. (A- B)	**2.11**	Total Th. (A- C)	**3.85**

4.2.3 Glow curve analysis

TLDs emit visible light while being heated by the TLD reader, the amount of light emitted at each temperature differs according to the type and composition of the TLD chip, the nature of the radiation dose, and the heating rate of the reader. In this study, it is shown that the TLD-600 neutron dose peaks are shown at the start of the heating, also known as the low temperature region, it is normally expected that pure photon irradiation yields a peak at higher temperature region, however in this study only a large peak is shown in the low temperature channels. A limitation of this is that low temperature peaks are prone to fading, and thus should either be read consistently early post-irradiation or the fading must be compensated for[25]. Glow curve deconvolution analysis of the peaks was performed using Origin software[26] to obtain individual curve readings, for this, a Gauss peak fit was used with a maximum of 200 iterations. Equation 7 describes the parameters of the four peaks that were discriminable. The R^2 value for TLD-600 peak fit was 0.9923 and for TLD-700 it was R^2= 0.9681, the reason for this difference in TLD-700 may be due to the fact that TLD-700 curves are very low in intensity and show some noise. Glow curve readingsof TLD-600 is shown in figure 13, figure 14 shows the deconvoluted glow curve for TLD-700 readings.

Equation 7 describes the glow curve, parameters y0, xc, w, A describe the behavior of Fit Peaks 1,2,3, and 4 in TLD-600 and TLD-700, these values are different depending on TLD type.

$$y = y0 + \frac{A}{w\sqrt{\frac{\pi}{2}}} \exp\left(-2\left(\frac{x - xc}{w}\right)^2\right)$$

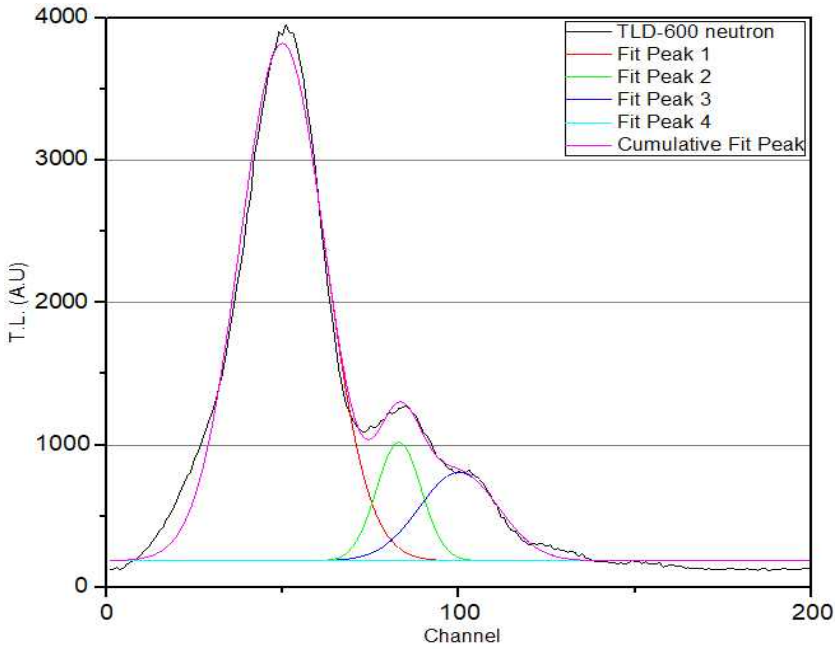

Figure 13deconvoluted glow curve of TLD-600 signal

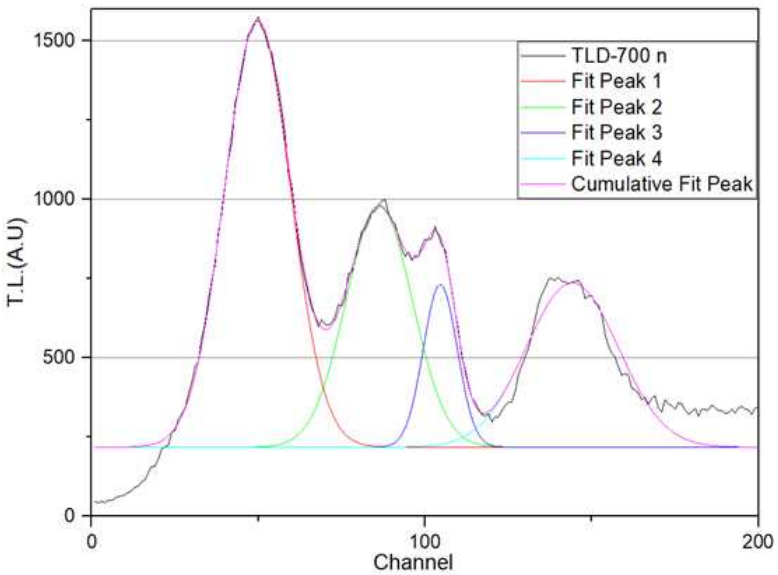

Figure 14deconvoluted glow curve of TLD-700 signal

4.3 Analytic calculation

As previously stated in chapter 2.1, the dose to TLD can be analytically calculated using equation 2, the dose in TLD resulting from the calculation would be in MeV/g, wherein the inputs are:

Q_1 = 4.78 MeV, is the energy released from $^6\mathrm{Li}(n,\alpha)$reaction,

ρ_1 = 2.55 g/cm^3, is the density of the TLD-600 chip,

N_{Li-6} = 6.211× 10^{22} atom/cm^{3}the atomic number density of ^{6}Li in TLD-600,

$\overline{\boldsymbol{\sigma}}^A = 539.39\times10^{-24}$, $\overline{\boldsymbol{\sigma}}^B = 556.97\times10^{-24}$, $\overline{\boldsymbol{\sigma}}^C = 555.07\times10^{-24}$, is the spectrum weighted cross-section for TLD-600 at position A, B and C.

$\Phi^A = 3.32\ \mathrm{n/cm^2/s}$, $\Phi^B = 1.55\ \mathrm{n/cm^2/s}$, $\Phi^C = 0.0825$ n/cm²/sis the thermal neutron flux for TLD in positions A,B, and C respectively as obtained using Monte Carlo Calculations

The dose was calculated according to these parameters. Table 6 shows a comparison between the analytically calculated energy depositions compared with simulated values obtained using F6 tally. Due to the very low thermal neutron fluence in TLDs at position C, despite using a large number of histories, the statistical uncertainty in MCNP simulation remained high due to the low number of neutrons making it in the TLD at position C, hence the large percent difference. This also demonstrates the

excellent shielding capability of the cadmium sheet to thermal neutrons. Table 6 shows the difference between the simulated neutron dose calculated from simulated energy deposit in MeV/g (for energies below 0.4 eV) and the analytically calculated energy deposition in units of MeV/g then converted to units of mGy for the total dose in TLD-600 chips during the whole irradiation period for TLDs at positions A, B, and C.

Table 6 a comparison between simulated and calculated neutron dose at TLDs in positions A, B, and C.

-	**Total simulated neutron dose in TLD-600 (in mGy)**	**Ratio (Normalized to A)**	**Calculated total neutron dose (in mGy)**	**Ratio (Normalized to A)**	**% difference**
A	1.653	**1.000**	1.385	**1.000**	**17.6 %**
B	0.7331	**0.443**	0.6680	**0.482**	**9.29 %**
C	0.01331	**0.00805**	0.04306	**0.0311**	**105%**

Discussion

The result of this work show that thermoluminescence dosimeters are suitable for thermal neutron fluence estimation with reasonable accuracy, this is done by comparing simulated neutron fluence and energy deposit in MCNP, converting the neutron fluence to ambient dose equivalent according to ICRP recommendations and then verifying it with experimentally obtained values using ICRP calibrated neutron probe. This method may be an appropriate alternative to activation foil method if TLDs uncertainty is accounted for. By using many TLDs, it is possible to obtain better statistics, Accounting for fading of the TLD signal must be accounted for by either consistently reading the TLDs after a consistent time interval or compensating for it. This pioneering research proved the concept is accurate enough but is has not yet fully established itself; therefore, more research should be done in different fields with different neutron spectra and different photon/neutron fluence ratios and intensities.

It is theoretically possible to estimate the neutron dose in lithium, boron, or nitrogen by knowing the neutron fluence and cross-section of the material using equation 1. By calculating the spectrum weighted cross-section of ^{10}B, ^{14}N cross-sections and using the simple ratio method, it is possible to obtain the slope of the cross-section of these elements and then knowing the imparted neutron dose.

In the thermal neutron range below 0.1 eV, the cross-section of ^{6}Li (473 barn) is higher than that of ^{197}Au (58.2 barn) –gold used in activation foils- indicating that ^{6}Li is theoretically more responsive to thermal neutrons than gold, also, unlike ^{197}Au, ^{6}Li does not show neutron resonance peaks in the fast neutron energy range so it is less responsive to fast neutrons. Realistically however, the sensitivity of each method depends on many variables such as the sensitivity of the reader, the signal of the irradiated sample, and the reading procedure.

This study used 160 TLDs to obtain higher statistics from the low neutron dose. Some 5 TLDs (out of 160 TLD) showed abnormal deviation from the mean. It may be postulated that these TLDs are either affected by alpha particles emitted from the (n, α) reaction of nearby TLDs that impart dose on neighboring TLDs, or, it might be due to some adhesive remaining from the tape used to hold the TLDs despite the efforts made to insure TLDs were clean and proper. The same TLDs were irradiated using an X-RAD-320 x-ray irradiation machine to 0.1 Gy at 120 kVp to investigate whether those TLDs are naturally over responsive, however, when read they showed no overresponse in photon irradiation, thus, it may be theorized that those TLDs' abnormal readings may have been affected by the alpha particles of neighboring TLDs.

A limitation of the study arises with human error, the quality of the TLDs and their reading deviation. The emitted signal from TLD is proportional to the neutron dose, however, TLDs show linearity from 10μGy to 1 Gy and supralinearity at doses above 1 Gy[15], this should be kept into account,also, any errors in the simulation leads to incorrect estimation of the neutron fluence, thus exercising proper documentation and experimental verification are necessary.

Conclusion

Neutron dose measurement and thermal neutron contribution fluence from a californium-252 were successfully quantified and measured by subtracting the reading of neutron insensitive TLD-700 from neutron sensitive TLD-600, the result eliminates the photon contribution leaving only neutron dose contribution. The experimentally obtained neutron dose contribution was compared with an MCNP simulation of the same irradiation room geometry to tally the neutron fluence and neutron energy deposit. The experimental results of the dose reading of TLDs directly irradiated by the moderated neutrons(position A),shielded in the front by a cadmium sheet (position B), and shielded by a folded cadmium pocket (position C) were evaluated,the ratios between theseshows a strong correlation when compared with the simulated neutron energy deposit in TLDs of similar geometry to within<5%. MCNP simulation of neutron fluence were experimentally verified using calibrated ^{3}He neutron probe and matched the ambient dose rate to within <3.5%. This proves the correctness and accuracy of this method, also, the simulated neutron fluence's ambient dose rate agrees well with the calibrated instrument's experimental reading.To further prove the simulation, the simulated neutron dose on the TLDs is also comparable to the analytically calculated values. It is possible to calibrate the TLDs using Monte Carlo simulated

neutron flux, provided that the latter are experimentally verified against calibrated instrument such as ^{3}He neutron probe. In this work, the proximity of TLD-600 chips near each-other during irradiation caused spurious readings in a few TLDs, shielding the TLDs against alpha particles induced from neutron irradiation is necessary for in-air irradiation setup.It is concluded that this method may be an acceptable alternative to the gold foil activation method in estimating thermal neutron fluence and that a cadmium sheet is sufficiently usable for thermal neutron fluence measurement even in case ofmixed-field dosimetry.

References

1. IAEA, *Current status of neutron capture therapy*, IAEA-TECDOC-1223, Editor. 2001, IAEA.
2. ICRP, *the 2007 Recommendations of the International Comission on Radiological Protection.* 2007. **1**(1): p. 17.
3. M.B. Chadwick, M.H., P. Obložinský, M.E. Dunn, Y. Danon, et al, G.M.Hale, P.G.Young, et al. , *ENDF/B-VII.1, Evaluated Nuclear Data Files,* .
4. Laboratory, L.L.N., *Neutron Sources for Standard-Based Testing*, L.L.N.L. Radoslav Radev Editor. 2014. p. 1-12.
5. Radoslav Radev , L.L.N.L., *Neutron Sources for Standard-Based Testing.* 2014: p. 3.
6. Laboratory, L.A.N., *MCNP6 User's Manual*. 2013.
7. Turner, J.E., *Atoms, Radiation, and Radiation Protection*. 2007.
8. Furetta, C., *Handbook of thermoluminescence, 2nd ed.* 2010.
9. *Conversion coefficients for Radiological Protection Quantities for External Radiation Exposures.* Ann, ICRP 40 (2-5), 2010.
10. Scientific, T. *TLD-600 Thermoluminescent Dosimetry Material*. Available from: https://www.thermofisher.com/order/catalog/product/SNO68815?SID=srch-srp-SNO68815.
11. Center, J.R., *A review of the recommendations for the Physical Dosimetry of Boron Neutron Capture Therapy (BNCT)*, W.P.V. G. G. Daquino, Editor. 2008.
12. A. L. Schwarz, R.A.S., L. L. Carter, *MCNP/MCNPX Visual Editor Computer code manual for Vised Version 24E.* 2011.
13. J., H.K., H.Park, K.-O. Choi, *Calibration of neutron personal doisimeters in a realistically simulated neutron irradiation room.* Radiation Measurements, 2010. **45**: p. 1544-1547.
14. Thiem Ngoc Le, H.-N.T., Khai Tuan Nguyen, Giap Van Trinh, *Neutron Calibration Field of a Bare 252Cf source in Vietnam.* Nuclear Engineering and Technology, 2017. **49**: p. 277-284.
15. Scientific, T.F., *Model 3500 Manual TLD Reader With WinREMS Operator's Manual*. 2010. p. 6-2.
16. B. Burgkhardt, G.F., A. Klett, A. Plewnia and B.R.L. Siebert, *The neutron fluence and H*(10) response of the new LB6411 remcounter* 1997: Radiation Protection Dosimetry. p. 361-364.
17. T. Goorley, e.a., *Initial MCNP6 Release Overview.* Nuclear Technology, 2012. **180**: p. 298-315.
18. J. K. Shultis, R.E.F., *An MCNP Primer*, K.s. university, Editor. 2006. p. 8.
19. Theis C., B.K.H., Brugger M., Forkel-Wirth D., Roesler S., Vincke H., , *Interactive three dimensional visualization and creation of geometries*

for Monte Carlo calculations. Nuclear Instruments and Methods in Physics Research 2006. **A562**: p. 827-829.
20. H Park, J.K., K. -O Choi, *Neutron calibration facility with radioactive neutron sources at KRISS.* Radiation protection and dosimetry, 2007. **126**(1-4): p. 159-162.
21. Knoll, G., *Radiation detection and measurements* 1999.
22. Bob D'Mellow, D.J.T., Malcolm J.Joyce, et al., *The replacement of cadmium as a thermal neutron filter.* Nuclear Instruments and Methods in Physics Research Section A, 2007. **577**(3): p. 690-695.
23. G. Gambarini, G.B., *Determination of gamma dose and thermal neutron fluence in BNCT beams from the TLD-700 glow curve shape.* Radiation Measurements, 2010. **45**(3-6): p. 640-642.
24. Taylor, J.R., *An introduction to Error Analysis: The Study of Uncertainties in Physical Measurements*. 1997.
25. Bircron, H., *LiF:Ti,Mg Methodology Guidelines for glow curve analysis.* 1991.
26. OriginLab Corporation, N., MA, USA., *Origin(Pro)*. 2016, b.

Appendix A

```
c ********************************************************************
c                    Cell Cards
c ********************************************************************
c 17 airbox
1  1 -1.204E-3 1 2 3 4 5 6 7 8 9 10 11 12 13 14 15 16 18 19 20 21
      23 24 25 26 27 28 29 30 -17  IMP:N,P,E,H = 1
c 22 outeredge concrete
2  22 -2.35 -22 17 IMP:N,P,E,H = 1
c 25 shield steel
3 14 -7.8  -25 24 IMP:N,P,E,H = 1
c 27 source rod
4  4 -7.8  -27 23 24 IMP:N,P,E,H = 1
c 23 source plate
5  6  -2.7 -23 27 26 IMP:N,P,E,H = 1
c 26 source
6  6  -2.6  -26 23 IMP:N,P,E,H = 1
c 12 cone pole
7  6 -2.7  -12  IMP:N,P,E,H = 1
c 5 steel cone
8  4 -7.8  -5  IMP:N,P,E,H = 1
c 3 Polyethylene cone
9  16 -0.95  -3  IMP:N,P,E,H = 1
c 28 stage car
10  4 -7.8  -28  IMP:N,P,E,H = 1
c 18 leg1
```

11 4 -7.8 -18 28 IMP:N,P,E,H = 1

c 19 leg2

12 4 -7.8 -19 28 IMP:N,P,E,H = 1

c 20 leg3

13 4 -7.8 -20 28 IMP:N,P,E,H = 1

c 21 leg4

14 4 -7.8 -21 28 IMP:N,P,E,H = 1

c 29 stagetop2

15 4 -7.8 -29 IMP:N,P,E,H = 1

c 4 PMMApole

16 25 -1.17 -4 IMP:N,P,E,H = 1

c 15 holderbase

17 23 -1.25 -15 IMP:N,P,E,H = 1

c 13 holdera

18 23 -1.25 -13 15 IMP:N,P,E,H = 1

c 14 holderb

19 23 -1.25 -14 15 IMP:N,P,E,H = 1

c 1 Cdsheet

20 17 -8.65 -1 IMP:N,P,E,H = 1

c 30 stagetoplow

21 23 -1.25 -30 4 IMP:N,P,E,H = 1

c 16 holdertop

22 23 -1.25 -16 IMP:N,P,E,H = 1

c 24 shieldinner

23 16 -1.0 -24 IMP:N,P,E,H = 1

c 2 Cdsheetfoldd

24 17 -8.65 -2 IMP:N,P,E,H = 1

c 8 TLD6pocket

25 20 -2.55 -8 IMP:N,P,E,H = 1

```
c 11 TLD7Ppocket
26  19 -2.65  -11  IMP:N,P,E,H = 1
c 9 TLD6p
27  20 -2.55  -9  IMP:N,P,E,H = 1
c 10 TLD7
28  19 -2.65  -10  IMP:N,P,E,H = 1
c 6 TLD6
29  20 -2.55  -6  IMP:N,P,E,H = 1
c 7 TLD7p
30  19 -2.65  -7  IMP:N,P,E,H = 1
c Explicit Blackhole/Universe
31  0  22 IMP:N,P,E,H = 0

c ***************************************************************************
c                    SurfaceCards
c ***************************************************************************
c
c 1 Cd sheet
1 BOX    519.50    191.50    195.50      0.10      0.00      0.00
        0.00      10.00      0.00      0.00      0.00      10.00
c 2 Cdsheet pocket
2 BOX    519.80    191.60    195.50      0.10      0.00      0.00
        0.00      4.00      0.00      0.00      0.00      10.00
c 3 Polyethcone
3 TRC 470.00 203.00 200.00
    35.00 0.00 0.00
    12.00 20.00
c 4 PMMApole
4 RCC 520.00 190.00 200.00 0.00 -65.00 0.00 2.00
```

c 5 steelcone

5 TRC 455.00 203.00 200.00

15.00 0.00 0.00

10.00 12.00

c 6 TLD-600

6 RCC 519.70 204.00 198.50 0.09 0.00 0.00 0.23

c 7 TLD-600 P

7 RCC 519.70 198.50 198.50 0.09 0.00 0.00 0.23

c 8 TLD-600pocket

8 RCC 519.70 194.00 198.70 0.09 0.00 0.00 0.23

c 9 TLD-700 P

9 RCC 519.70 198.50 202.50 0.09 0.00 0.00 0.23

c 10 TLD-700

10 RCC 519.70 204.00 202.50 0.09 0.00 0.00 0.23

c 11 TLD-700pocket

11 RCC 519.70 194.00 202.50 0.09 0.00 0.00 0.23

c 12 coneholdingpole

12 RCC 470.00 190.00 200.00 0.00 -140.00 0.00 2.00

c 13 holdera

13 BOX 519.10 191.00 196.00 0.30 0.00 0.00

0.00 16.00 0.00 0.00 0.00 0.30

c 14 holderb

14 BOX 519.00 191.00 205.00 0.30 0.00 0.00

0.00 16.00 0.00 0.00 0.00 0.30

c 15 holderbase

15 BOX 519.00 191.00 195.00 2.00 0.00 0.00

0.00 0.50 0.00 0.00 0.00 11.00

c 16 holdertop

16 BOX 519.00 207.00 195.85 0.30 0.00 0.00

```
        0.00      0.50      0.00      0.00      0.00      9.50
c 17 innerroom
17 BOX    -62.00      0.00    -75.00    830.00      0.00      0.00
        0.00    410.00      0.00      0.00      0.00    640.00
c 18 leg1
18 BOX    515.00    100.00    195.00      1.00      0.00      0.00
        0.00     25.00      0.00      0.00      0.00      1.00
c 19 leg2
19 BOX    515.00    100.00    205.00      1.00      0.00      0.00
        0.00     25.00      0.00      0.00      0.00      1.00
c 20 leg3
20 BOX    525.00    100.00    205.00      1.00      0.00      0.00
        0.00     25.00      0.00      0.00      0.00      1.00
c 21 leg4
21 BOX    525.00    100.00    195.00      1.00      0.00      0.00
        0.00     25.00      0.00      0.00      0.00      1.00
c 22 outerworld
22 BOX   -112.00    -50.00   -125.00    930.00      0.00      0.00
        0.00    510.00      0.00      0.00      0.00    750.00
c 23 source plate
23 RCC 420.00 200.00 200.00 0.00 -2.00 0.00 6.00
c 24 shieldPE
24 RCC 420.00 150.00 200.00 0.00 -100.00 0.00 25.00
c 25  shieldsteel
25 RCC 420.00 150.00 200.00 0.00 -100.00 0.00 30.00
c 26 source
26 RCC 420.00 203.00 200.00 0.00 -3.00 0.00 1.00
c 27 sourcerod
27 RCC 420.00 198.00 200.00 0.00 -50.00 0.00 2.00
```

```
c 28 stagecar
28 BOX     500.00     100.00     175.00     100.00       0.00       0.00
         0.00       1.00       0.00       0.00       0.00      50.00
c 29 stagetop2
29 BOX     515.00     190.00     195.00      11.00       0.00       0.00
         0.00       1.00       0.00       0.00       0.00      11.00
c 30 stagetoplow
30 BOX     515.00     125.00     195.00      11.00       0.00       0.00
         0.00       1.00       0.00       0.00       0.00      11.00

c ***************************************************************************
c                    Materials
c ***************************************************************************
c
m1    7014.70c       -0.7548  $ Air
      8016.70c       -0.232
      18000.35c      -0.0132
m4    6000.70c       -0.0003  $ 304L Stainless Steel
      24000.50c      -0.19 28000.50c    -0.095 26000.55c    -0.7147
m6    13027.70c      -0.9792  $ 6061-T6 Aluminium
      14000.51c      -0.006  29000.50c    -0.0028 12000.51c      -0.01
      24000.50c      -0.002
MT6 al27.12t
m14   26000.55c          1  $ Iron
MT14 fe56.12t
m16   1001.70c           2  $ P.E(DENSITY = -0.95 g/cm^3)
      6000.70c           1  $ 6000.70c is correct
MT16 poly.10t
m17   48000.42c         1  $ Cd (assumption, Density = -8.65 g/cm^3)
```

```
m19   3007.70c   -0.26490
      9019.70c  -0.732
      3006.70c  -0.00267 $ TLD7 d=2.65
m20  3006.70c   -0.25581126 $ tld-600 d=2.55
     9019.70c   -0.732415
     3007.70c   -0.01177374
m22  1001.70c   -0.008485 $ concrete
     6000.70c   -0.050064
     8016.70c   -0.473483
     12024.70c  -0.024183
     13027.70c  -0.036063
     14028.70c  -0.1451
     16032.70c  -0.00297
     19039.70c  -0.001697
     20040.70c  -0.246924
     26054.70c  -0.011031
m23  1001.70c 4  $ PLA d=1.25 g/cc
     6000.70c 3
     8016.70c 2
MT23 poly.10t
c m24  98252.70c 1 $ Cf source
m25  6000.70c 5 $ PMMA d=1.18 g/cc
     8016.70c 2
     1001.70c 8
MT25 poly.10t
c END OF MATERIALS
C DATA CARDS
sdef par=n pos=420 202 200   erg=d1
sp1  -3  1.025   2.926  $  Cf-252, watt fission
```

```
phys:n
mode n
c ====================== Tally definition, conversion coeff ================
c Cd sheet
c below are dose tallies
df0  99 fac=-3
fc6 Neutron energy deposition MeV/g for tld-600
f6:n 29
e6 1.00E-09  1.00E-08  2.53E-08  1.00E-07  2.00E-07  5.00E-07  1.00E-06
    2.00E-06  5.00E-06  1.00E-05  2.00E-05  5.00E-05  1.00E-04  2.00E-04
    5.00E-04  1.00E-03  2.00E-03  5.00E-03  1.00E-02  2.00E-02  3.00E-02
    5.00E-02  7.00E-02  1.00E-01  1.50E-01  2.00E-01  3.00E-01  5.00E-01
    7.00E-01  9.00E-01  1.00E+00  1.20E+00  2.00E+00  3.00E+00  4.00E+00
    5.00E+00  6.00E+00  7.00E+00  8.00E+00  9.00E+00  1.00E+01  1.20E+01
    1.40E+01  1.50E+01  1.60E+01  1.80E+01  2.00E+01
fc26 Neutron energy deposition MeV/g for really  tld-600P
f26:n 27
e26 1.00E-09  1.00E-08  2.53E-08  1.00E-07  2.00E-07  5.00E-07  1.00E-06
    2.00E-06  5.00E-06  1.00E-05  2.00E-05  5.00E-05  1.00E-04  2.00E-04
    5.00E-04  1.00E-03  2.00E-03  5.00E-03  1.00E-02  2.00E-02  3.00E-02
    5.00E-02  7.00E-02  1.00E-01  1.50E-01  2.00E-01  3.00E-01  5.00E-01
    7.00E-01  9.00E-01  1.00E+00  1.20E+00  2.00E+00  3.00E+00  4.00E+00
    5.00E+00  6.00E+00  7.00E+00  8.00E+00  9.00E+00  1.00E+01  1.20E+01
    1.40E+01  1.50E+01  1.60E+01  1.80E+01  2.00E+01
fc36 Neutron energy deposition MeV/g for tld-600 + 2Cd
f36:n 25
e36 1.00E-09  1.00E-08  2.53E-08  1.00E-07  2.00E-07  5.00E-07  1.00E-06
    2.00E-06  5.00E-06  1.00E-05  2.00E-05  5.00E-05  1.00E-04  2.00E-04
    5.00E-04  1.00E-03  2.00E-03  5.00E-03  1.00E-02  2.00E-02  3.00E-02
```

5.00E-02 7.00E-02 1.00E-01 1.50E-01 2.00E-01 3.00E-01 5.00E-01

7.00E-01 9.00E-01 1.00E+00 1.20E+00 2.00E+00 3.00E+00 4.00E+00

5.00E+00 6.00E+00 7.00E+00 8.00E+00 9.00E+00 1.00E+01 1.20E+01

1.40E+01 1.50E+01 1.60E+01 1.80E+01 2.00E+01

fc46 Neutron energy deposition MeV/g for tld-700

f46:n 28

e46 1.00E-09 1.00E-08 2.53E-08 1.00E-07 2.00E-07 5.00E-07 1.00E-06

2.00E-06 5.00E-06 1.00E-05 2.00E-05 5.00E-05 1.00E-04 2.00E-04

5.00E-04 1.00E-03 2.00E-03 5.00E-03 1.00E-02 2.00E-02 3.00E-02

5.00E-02 7.00E-02 1.00E-01 1.50E-01 2.00E-01 3.00E-01 5.00E-01

7.00E-01 9.00E-01 1.00E+00 1.20E+00 2.00E+00 3.00E+00 4.00E+00

5.00E+00 6.00E+00 7.00E+00 8.00E+00 9.00E+00 1.00E+01 1.20E+01

1.40E+01 1.50E+01 1.60E+01 1.80E+01 2.00E+01

fc66 Neutron energy deposition MeV/g for really tld-700P

f66:n 30

e66 1.00E-09 1.00E-08 2.53E-08 1.00E-07 2.00E-07 5.00E-07 1.00E-06

2.00E-06 5.00E-06 1.00E-05 2.00E-05 5.00E-05 1.00E-04 2.00E-04

5.00E-04 1.00E-03 2.00E-03 5.00E-03 1.00E-02 2.00E-02 3.00E-02

5.00E-02 7.00E-02 1.00E-01 1.50E-01 2.00E-01 3.00E-01 5.00E-01

7.00E-01 9.00E-01 1.00E+00 1.20E+00 2.00E+00 3.00E+00 4.00E+00

5.00E+00 6.00E+00 7.00E+00 8.00E+00 9.00E+00 1.00E+01 1.20E+01

1.40E+01 1.50E+01 1.60E+01 1.80E+01 2.00E+01

fc76 Neutron energy deposition MeV/g for tld-700 + 2Cd

f76:n 26

e76 1.00E-09 1.00E-08 2.53E-08 1.00E-07 2.00E-07 5.00E-07 1.00E-06

2.00E-06 5.00E-06 1.00E-05 2.00E-05 5.00E-05 1.00E-04 2.00E-04

5.00E-04 1.00E-03 2.00E-03 5.00E-03 1.00E-02 2.00E-02 3.00E-02

5.00E-02 7.00E-02 1.00E-01 1.50E-01 2.00E-01 3.00E-01 5.00E-01

7.00E-01 9.00E-01 1.00E+00 1.20E+00 2.00E+00 3.00E+00 4.00E+00

5.00E+00 6.00E+00 7.00E+00 8.00E+00 9.00E+00 1.00E+01 1.20E+01

1.40E+01 1.50E+01 1.60E+01 1.80E+01 2.00E+01

PRDMP 5e8

nps 3e9

Abstract (Korean)

BNCT 시설,원자로,그리고다른중성자선원에서발생하는열중성자속의측정
(또는평가)이필요한경우주로방사화박을이용하게된다.그러나방사화박 (activation foils)은방사화붕괴시간에의한추가시간의소요,원하지않은물질의방사화에의한노이즈그리고방출되는광자계측을위한고가의 HPGe 계측기의필요로단점을나타낸다.

본연구의목적은 LiF 기반열형광선량계를이용하여다른방법으로열중성자속을측정및평가하는것에있다.이방법은의료계에서광자와중성자를측정하는것에널리사용되고반응도와특성이잘파악되어있는열형광선량계를이용함으로흔히사용되지만복잡한방법론과고가의장비를필요로하는방사화박을대체할수있다.

본연구는몬테카를로계산을이용하여감속물질(그림자원뿔, shadow cone) 을통과한 Cf-252 중성자선원에서나온열중성자를평가하고,실험적으로중성자속,선량축적량그리고 H*(10)

주위선량당량을측정한다.열중성자를설명하기위해카드뮴시트를접어열형광선량계에직접적으로입사하는중성자와튕겨져입사하는중성자를나누었다.열중성자속은카드뮴시트를이용하여열중성자를막은그룹과막지않은그룹의측정값에서단순히차이를구하는것으로알아낼수있었는데,

이는카드뮴이열중성자를높은확률로막을수있기때문이다.감속물질은 Cf-252 선원과열형관선량계사이에위치하였고,Cf-252 에서발생한고속중성자를열중성자화하는역할을하였다.

몬테카를로계산에의하면열형광선량계에축적된에너지의대부분은열중성자에의한것이었고,열중성자중에서조사실벽에서튕겨져나온중성자의영향이반드시고려를해야할만큼컸다.열중성자속또한몬테카를로시뮬레이션을이용하여추정하고, H*(10) 주위선량당량으로변환되었으며,교정된 ^{3}He 계측기의값으로검증하여 3.5% 이내의차이를확인했다.위치 A (Cd 시트없음), B (한쪽면을 Cd 시트로방호), C (접은 Cd 시트를사용하여양쪽면방호)에서열중성자속과열중성자속비율의몬테카를로계산결과는열형광선량계로측정한값과잘맞았고해석적인계산값또한잘맞았다.

결론으로,본연구에서개발된방법이열중성자속을측정하는목적으로기존의방사화박방법을대체하기에충분하였다.몬테카를로시뮬레이션결과가측정결과와잘맞았기때문에추후열형광선량계시스템을교정하는데이러한방법이사용될수있을것이다.